A LIGHTWEIGHT PAYLOAD FOR HYPERSPECTRAL REMOTE SENSING USING SMALL UAVS

João Fortuna and Tor Arne Johansen

Centre for Autonomous Marine Operations and Systems (NTNU AMOS)
Department of Engineering Cybernetics, Norwegian University of Science and Technology (NTNU)
Trondheim, Norway

ABSTRACT

In this paper we describe a lightweight hyperspectral imaging payload consisting of a push-broom imager, GPS and IMU sensors as well as data synchronization and acquisition systems. The payload is developed in a modular and customizable way, making it a flexible UAV payload for research activities.

We will present the hardware and software set up, with details on each of the components and their interaction. Finally we show results from field tests.

***Index Terms*—** Hyperspectral, instrument, airborne, remote sensing, UAV

1. INTRODUCTION

Airborne hyperspectral data provides a wealth of information currently used in fields such as agriculture, environmental monitoring and protection, and infrastructure inspection, just to name a few. For such applications, the spectral range is usually 400-1000nm, commonly referred to as VNIR (visible and near-infrared).

Some producers of hyperspectral sensors also provide complete systems that can fit in a small UAV: Specim's AisaKESTREL10 [1] offers a 400-1000nm range, 2048 pixels spatial resolution at a <5kg total system weight; Resonon's Airborne Hyperspectral Imaging Systems [2] can be customized with their different cameras. When using the Pika L model, the spectral range is also 400-1000nm, with 900 spatial pixels at <1.5kg for the total system; or the new Nano-Hyperspec sensor by Headwall [3] with the same spectral range of 400-1000nm, spatial resolution of 640 pixels and <0.52kg without lens.

The Unmanned Aerial Vehicles Laboratory (UAV-Lab) at the Norwegian University of Science and Technology (NTNU) is focused on developing smaller low cost and open-source tools while still aiming at high performance. With that in mind, we developed the payload here described. Specifications will be further detailed, but as a quick comparison to the mentioned systems we provide 400-950nm and 580 spatial pixels at 152g instrument weight.

(a) Standalone. (b) Mounted on Maritime Robotics' hexacopter.

Fig. 1: Prototype payload.

The next section provides an overview of the system, detailing the choice of each component and how it was integrated in the payload. Then, we present experimental results obtained in flight, followed by a few concluding remarks.

2. SYSTEM OVERVIEW

The described payload, Figure 1a, is a highly modular system: sensors can be added, removed or swapped. All changes have of course an impact on the quality of the final data product. E.g. having a lower performance, but cheaper GPS will produce less accurate georeferencing. In this paper we present the current version of the payload's set up.

Figures 2 and 3 show the data and power flow, respectively. In dark color are data or power sources, in white the conversion or routing elements and finally in a light color are data storage/transmission or power consuming components. The following sections will explain each component interaction in more detail.

2.1. SenTiBoard

The **Sen**sor **Ti**ming **Board** provides accurate timestamps with a 10ns resolution for all sensors. This component is described in [4][5]. By using data from the IMU and GPS sensors and a navigation filter [6], we can generate georeferenced maps of hyperspectral data.

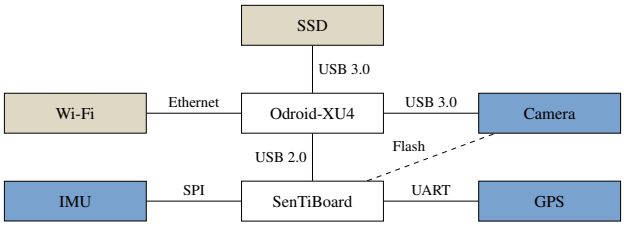

Fig. 2: Data connection diagram.

2.2. Hyperspectral Instrument

In the heart of our system is the push-broom [7] hyperspectral instrument. This model was developed using 3D printed parts and commercial off-the-shelf (COTS) optical components and the optics are discussed in detail in [8]. By developing the system in such way that the camera can be chosen with some degree of freedom, it allowed us to select a model with the required spectral sensitivity as well as easy Linux integration.

2.2.1. Camera

The camera model used in the current version of the system is the UI-3360CP-NIR-GL, with enhanced NIR sensitivity, produced by IDS Imaging Development Systems GmbH [9]. This corresponds to model **C**, refer to Section 4 in [8]. Raw data depth is 12 bit, it provides a USB 3.0 interface for data transfer, and an 8-pin I/O connector with flash signal, trigger and GPIO pins.

2.2.2. Optics

The principle used for hyperspectral imaging is a push-broom instrument. This is achieved through the use of a slit, a dispersing element (grating), and required focusing lenses [8]. Because this camera was developed using COTS components, the available slits did not allow taking advantage of the full size of the sensor. While the sensor has 1088 pixels in the spatial axis, we can only use 580.

The spectral range of the instrument is theoretically 300-1000nm, however wavelengths below 400nm are blocked by the glass lenses, and in addition, frequencies above 800nm suffer from blending with the second spectral order [8]. Despite these limitations we record the 350-950nm range so we can later decouple some of these effects in post processing.

The ground resolution is given by:

$$d_x = \frac{z \times w}{f_1} \quad [m] \tag{1}$$

$$\Delta_x = d_x + v \times \Delta_t \quad [m] \tag{2}$$

$$\Delta_y = \frac{z \times h}{f_1 \times N} \quad [m] \tag{3}$$

Where $f_1 = 16mm$ (front lens focal distance), $w = 25\mu m$ (slit width) and $h = 3mm$ (slit height) [8]. The remaining variables: $N = 580$ (usable pixels in spatial axis) was discussed before, then z (flight altitude), v (ground speed) and Δ_t (exposure time) can be changed in each flight.

2.2.3. Data acquisition

To enable the synchronization of the camera frames to the rest of the data, the flash output signal is fed to the SenTiBoard. Figure 4 shows the wiring schematic used to capture the flash signal, as recommended in the camera manual [10]. The signal in the Time of Validity (TOV) node will be high (5V) whenever the flash is active, and low (GND) otherwise. When initializing the camera, we configure the flash to be active for the entire duration of the exposure time. The SenTiBoard will record the time of every falling-edge (transition from 5V to GND) in TOV, thus timestamping the end of each exposure.

Due to limitations in processing power and writing speed in the on-board computer, we perform *off-chip* spectral binning [7] on the frames before saving to disk. The binning operation reduces the size of the image by adding columns together. After experimenting with different settings, a value of $10\times$ seems to allow recording data at 30fps. Since the raw data is captured at 12 bit depth, it is possible to bin up to $16\times$ without risking overflow when using a 16 bit image container file. The chosen binning factor results in a spectral resolution of approximately 4nm per band. Because of the limited usable spatial and spectral ranges caused by the optics, we only read a cropped area of the sensor that is 1800×600 pixels. When applying $10\times$ spectral binning to those frames we end up with 16 bit images of 180×600 pixels that should be stored.

2.2.4. Calibration

Our instrument was wavelength calibrated to match pixels in the spectral axis to actual wavelengths. The procedure used was to point the camera to a fluorescent light tube with known sharp emission bands [11] and capture data. Then, visually match the peaks to those bands as seen in Figure 5. Finally, fit a second degree polynomial on the pixel-wavelength pairs discovered, as mentioned in Section 5 of [12].

Radiometric calibration was not performed, as we are still testing the sensor to find optimal settings.

2.3. Other Hardware

2.3.1. Navigation Sensors

For high positioning accuracy, we used an RTK (Real Time Kinematic) capable GPS module. The model selected was uBlox-NEO-M8T, assembled on a breakout board by CSG Shop [13]. We time and log the following messages: RXM-RAWX, RXM-SFRBX, NAV-PVT as per the instructions in [5].

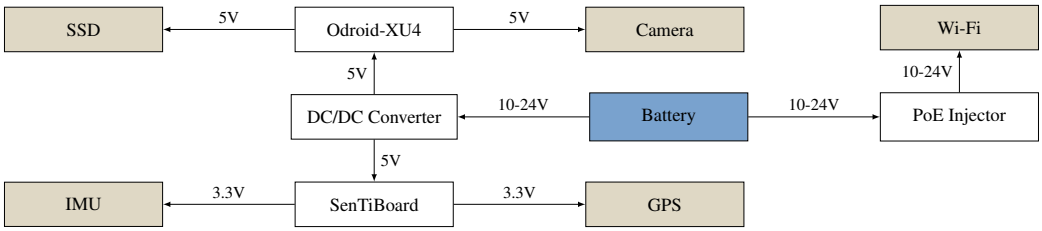

Fig. 3: Power distribution diagram.

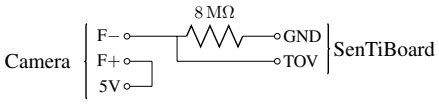

Fig. 4: Flash electrical wiring.

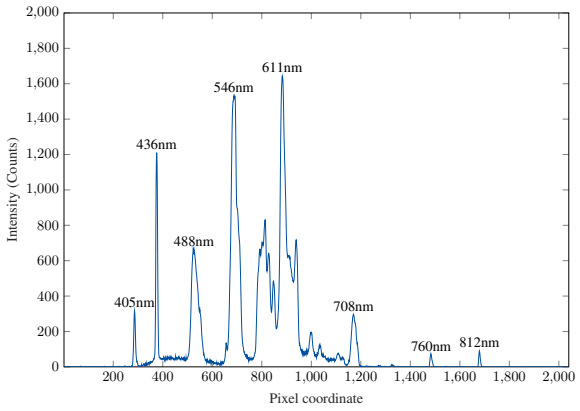

Fig. 5: Fluorescent light spectrum.

The chosen IMU was the ADIS16490 3-axis gyroscope and accelerometer.

There is no heading sensor installed in this version of the payload, but heading information can be retrieved from the UAV autopilot logs. Timing is synchronized through GPS times both on the payload and autopilot.

2.3.2. *On-board computer*

As this system is to be used for small scale UAV-based airborne surveys, there was need to have an on-board computer that can acquire and log data. We chose the Odroid-XU4 board [14]. This board is also recommended by the camera manufacturer for embedded applications.

To accommodate for the high data rate coming from the camera, we opted for a USB 3.0 SSD disk. Initial tests with USB flash drives and μSD cards showed that those devices were not fast enough.

2.3.3. *Communications*

In its stand-alone version, the payload includes a Wi-Fi radio for communication. During the field experiments this radio was configured as an Access Point (hotspot), this way we could connect to it using the integrated network card on a laptop. Data rate requirements are low, as external communication is used only for status monitoring and acquisition control.

2.4. Software

One of our goals when developing this payload was to make it as easy to use as possible. By simplifying and automatising the acquisition process, field experiments can be made more efficient. We achieve this by using the *LSTS Toolchain* [15], an open-source project with a suite of tools for autonomous systems that include on-board control and logging (DUNE), communication protocol (IMC) and a graphical user interface (Neptus) for mission control and log analysis. The UAV-Lab has contributed to and used this toolchain in the past [16], thus making it the prime candidate for powering our system.

DUNE [17] is the software running on the on-board computer. It manages the activation and logging of the sensor data, as well as communication with the ground station. To support the chosen hardware there was a need to develop two "Tasks" in DUNE: one for interfacing the camera and another for the SenTiBoard.

3. EXPERIMENTAL RESULTS

On March 22nd, 2018 we flew over Hopavågen, a salt water pool in the Trøndelag region, Norway. This is an area of interest for the Department of Biology at NTNU, who provided us with the experiment goal of mapping different types of habitats in shallow water such as sea-grass, rocks, sand or sea-urchins. In the past, this has been performed manually.

The target to observe was underwater, and in addition on that day the sky was very cloudy. That resulted in non-ideal conditions. Before flight, ground tests were made to find the best settings for image capture. Table 1 shows the flight parameters and sensor configuration.

The payload was mounted on a hexacopter as seen in Figure 1b. During the flights an additional RGB camera was also capturing images. Data from both RGB and HS cameras are

Table 1: Experiment parameters.

Parameter	Value	Unit
Frame rate	20	frames/s
Exposure time	49.9 (max)	ms
Sensor Gain	4	-
Flight Altitude	10	m
Flight Speed	1.5	m/s

seen in Figure 6. The two images were matched manually based on timing information and ground features. Spectral data from each of the marked points of interest can be seen in Figure 7.

Using the values from Table 1 in Equations 1-3, we get ground resolutions per pixel of $\Delta_x \approx 90mm$ (along track) and $\Delta_y \approx 3mm$ (across track). Ground sampling distance is $v/fps = 75mm$.

4. FUTURE WORK

We are currently working on the final piece of the HS data acquisition and pre-processing pipeline: automatic georeferencing, map generation and GIS software compatibility. The first step towards it is the processing of raw navigation data into a full navigation solution [6].

Other features that should be added in the near future are the ability to change settings more easily, detection of relevant target signatures during flight, streaming of more detailed capture status and data quality diagnostics. In addition, we will perform radiometric and geometric calibration.

Regarding the mechanical assembly of the payload, the current solution is experimental. Once we decide on a fixed set of components we can design a custom enclosure with minimal weight and volume, while keeping the required mechanical and thermal stability.

5. CONCLUSIONS

Our system proved to be easy to use in the field, requiring little interaction beyond initial parameter setting.

Because of the grating-slit design of the push-broom camera the amount of light captured by the sensor is very limited, this sets some requirements on light/weather conditions during experiments. Changing flight parameters or the slit width can increase the amount of light, however that comes at the expense of reduced area coverage, spatial and/or spectral resolutions.

6. ACKNOWLEDGEMENTS

6.1. Author Contributions

João Fortuna wrote the core text, designed the payload with the available components, developed the necessary code for data acquisition and storage, as well as post-processing and visualization. In addition he performed the field experiments.

Tor Arne Johansen was the supervisor during the planning and execution phases, and later reviewer of this text.

6.2. Other Contributions

Fred Sigernes designed the optics and mechanical assembly of the hyperspectral camera that started this project. He also provided support on the calibration and interpretation of the resulting data.

Sigurd M. Albrektsen developed and produced the SenTiBoard and provided support during its integration in the payload.

Mechanical assembly was aided by Sivert Bakken, student at NTNU.

Geir Johnsen and Aksel Mogstad from the Department of Biology at NTNU provided an experimental scenario with scientific objectives.

Maritime Robotics and Pål Kvaløy, pilot at the UAV-Lab allowed us to field test the payload.

Torleiv H. Bryne was a valuable asset in all questions regarding the processing of navigation data.

6.3. Funding

This work was supported by the Norwegian Research Council (grant nos. 223254 and 221666) through the Centre of Autonomous Marine Operations and Systems (NTNU AMOS) at the Norwegian University of Science and Technology, the MASSIVE project (grant no. 270959), as well as the Norwegian Space Center.

7. REFERENCES

[1] "Specim - AisaKESTREL," 2018, http://www.specim.fi/products/aisakestrel-hyperspectral-imaging-system/.

[2] "Resonon - Airborne Hyperspectral Imaging Systems," 2018, https://www.resonon.com/Products/airborne.html.

[3] "Headwall - Nano-Hyperspec," 2018, http://www.headwallphotonics.com/spectral-imaging/hyperspectral/nano-hyperspec.

[4] S. M. Albrektsen and T. A. Johansen, "User-configurable timing and navigation for uavs," *Sensors*, vol. 18, no. 8, 2018.

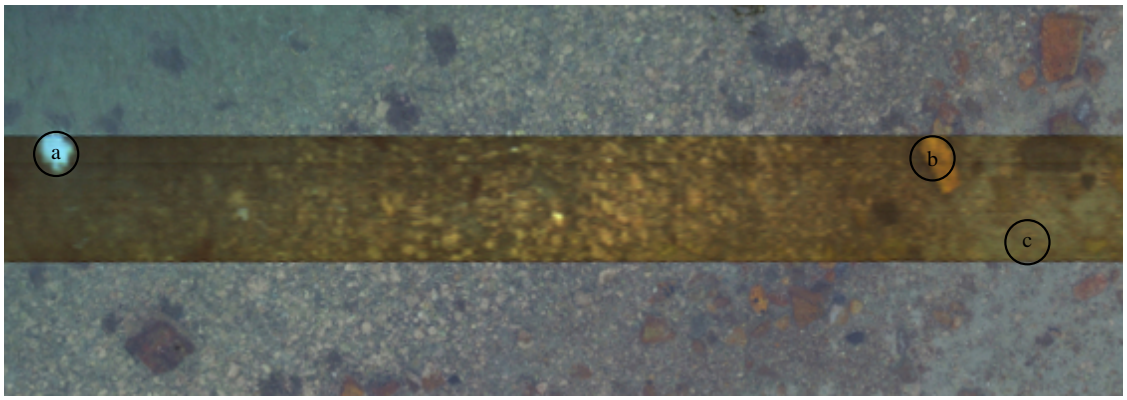

Fig. 6: Hyperspectral data (RGB rendering) overlayed on RGB image taken during flight. Swath width of HSI is 1.875m.

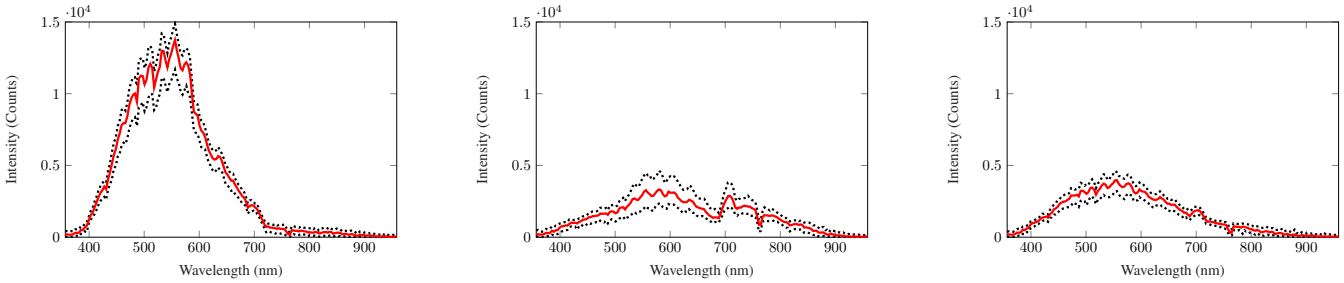

(a) White reference (b) Orange rock (c) Sand in shallow water

Fig. 7: Mean spectrum (red solid line) and range (dotted black line) for each point of interest.

[5] "SenTiBoard," 2018, https://sentiboard.com/.

[6] T. H. Bryne, J. M. Hansen, R. H. Rogne, N. Sokolova, T. I. Fossen, and T. A. Johansen, "Nonlinear Observers for Integrated INS/GNSS Navigation: Implementation Aspects," *IEEE Control Systems Magazine*, vol. 37, no. 3, pp. 59–86, June 2017.

[7] F. Dell'Endice, J. Nieke, B. Koetz, M. E. Schaepman, and K. Itten, "Improving radiometry of imaging spectrometers by using programmable spectral regions of interest," *ISPRS Journal of Photogrammetry and Remote Sensing*, vol. 64, no. 6, pp. 632 – 639, 2009.

[8] F. Sigernes, M. Syrjäsuo, R. Storvold, J. Fortuna, M. E. Grøtte, and T. A. Johansen, "Do it yourself hyperspectral imager for handheld to airborne operations," *Opt. Express*, vol. 26, no. 5, pp. 6021–6035, Mar 2018.

[9] "IDS - UI-3360CP Rev. 2," 2018, https://en.ids-imaging.com/store/ui-3360cp-rev-2.html.

[10] "uEye Camera Manual," 2018, https://en.ids-imaging.com/manuals/uEye_SDK/EN/uEye_Manual_4.90.3/index.html.

[11] "Wikipedia - Fluorescent lighting spectrum peaks labelled," 2018, https://commons.wikimedia.org/wiki/File:Fluorescent_lighting_spectrum_peaks_labelled.gif.

[12] F. Sigernes, "Airborne Hyperspectral Imaging," Tech. Rep., University Centre in Svalbard, 2002.

[13] "CSG Shop - InCase PIN series NEO-M8T TIME & RAW receiver board (RTK ready)," 2018, http://www.csgshop.com/product.php?id_product=240.

[14] "Hardkernel - Odroid-XU4," 2018, http://www.hardkernel.com/main/products/prdt_info.php?g_code=G143452239825.

[15] J. Pinto, P. S. Dias, R. Martins, J. Fortuna, E. Marques, and J. Sousa, "The LSTS toolchain for networked vehicle systems," in *2013 MTS/IEEE OCEANS - Bergen*, June 2013, pp. 1–9.

[16] A. Zolich, T. A. Johansen, K. Cisek, and K. Klausen, "Unmanned aerial system architecture for maritime missions," in *2015 Workshop on Research, Education and Development of Unmanned Aerial Systems (RED-UAS)*, Nov 2015, pp. 342–350.

[17] "DUNE: Unified Navigation Environment, GitHub reposiroty," 2018, https://github.com/lsts/dune.